

Behavior and Design of T-Section Thin-Walled Columns

Carina Filipa Gomes Caldeira

*Department of Civil Engineering, Architecture and Geo-Resources Superior Técnico, Universidade de Lisboa,
Avenida Rovisco Pais, 1, 1049-001 Lisboa, Portugal*

Abstract

This work presents and discusses the buckling, post-buckling and ultimate behaviour of centrally compressed thin-walled T-sections members. It is firstly presented a brief literature review on recent studies involving this type of columns, and secondly the stability analysis of a wide range of members, with both ends fixed and different cross sections dimensions, obtain through GBTUL code, based on the Generalized Beam Theory – the study made possible to characterize the column buckling modes and select the dimensions, namely the length of the members. Then, the elastic and elasto-plastic post-buckling behaviours of short-to-intermediate columns with different values tensile stresses is analysed, using ABAQUS code. Finally, based in a parametric study carried out to determine a wide range of ultimate load values, the quality of the Direct Strength Method (DSM) predictions to estimate the resistance of cold formed steel fixed-ended T section columns is assessed.

Keywords: Cold-formed steel columns; Local buckling; Global buckling; Post-buckling and ultimate behaviour; Direct strength method.

Introduction

Thin-walled members with cross-sections which have all their mid-lines intersected at a single point (e.g., angle-sections, T-sections and cruciform members) exhibit no primary warping resistance (only secondary warping), leading to a high susceptibility of those thin-walled members to buckling phenomena involving torsion (torsional or flexural-torsional buckling).

Moreover, in members with the above cross-section shape is difficult to distinguish between local and global buckling. These instability phenomena are usually associated with a distinct post-buckling behaviour, so the identification of the instability nature has important implications in the structural models used for the design of those members.

The buckling and post-buckling behaviour of those members attracted the attention of several researchers – e.g., the studies developed by (i) Dinis et al. [8], on the local and global buckling behaviour of angles, T-Sections and cruciforms columns, (ii) Leal [12], on members with T-sections obtained from dual angles connected by the legs, (iii) Sena Cardoso & Rasmussen [13], involving hot rolled profiles, and finally, (iv) the experimental investigation performed by Vishnuvardhan & Samuel Knight [14], involving cold formed steel single angles, double angles welded-back-to-back (T-sections) and starred angles under three different end connections.

Buckling Behaviour

The results of a parametric study carried out with the aim to characterize the mechanisms underlying the buckling behaviour of steel T section columns is performed, using GBTUL code – the importance of the flange and thickness dimensions is assessed (in particular of the web's thickness variation). However, only the results of the study assuming short flanges are presented. This study also enabled the selection of a set of profiles (cross-sectional dimensions and length), whose post-buckling behaviour will be analysed in the next chapter.

Figure 1 represents the deformation modes of column with T-sections. The modes (a), (b) and (c) regards to rigid body modes (major and minor axis flexure and torsion) and (d) and (e) are related to local modes.

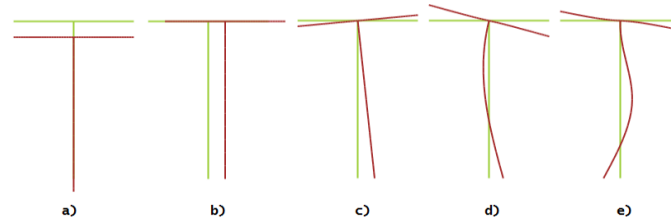


Figure 1: Mid-span cross-section deformed for T-sections columns. Modes (a) and (b) major and minor axis flexural, (c) torsion (d) and (e) local instability modes.

Table 1 and Table 2 presents the cross-sections analysed in this study. In a first approach, it was considered for both members a constant thickness equal to $t=1.2\text{mm}$ and later a web thickness equal to twice ($t_w = 2.4\text{ mm}$) of the flange dimension ($t_f = 1.2\text{ mm}$).

Table 1: Study sections properties with 1.2mm of thickness members.

| | T_1 | T_2 | T_3 | T_4 | T_5 | T_6 | T_7 |
|------------------|-------|-------|-------|-------|-------|-------|-------|
| $b_f(\text{mm})$ | 30 | 50 | 70 | 90 | 110 | 130 | 140 |
| $b_w(\text{mm})$ | 70 | 70 | 70 | 70 | 70 | 70 | 70 |

Table 2: Study sections properties with $t_w = 2.4\text{mm}$ and $t_f = 1.2\text{mm}$.

| | T_{12} | T_{32} | T_{72} |
|------------------|----------|----------|----------|
| $b_f(\text{mm})$ | 30 | 70 | 140 |
| $b_w(\text{mm})$ | 70 | 70 | 70 |

The parametric study on the buckling behavior of steel ($E = 210\text{ GPa}$ and $\nu = 0.3$) T-section columns, for each geometry indicated in previous tables, consisted in the change of the column length in small ranges, between 200 and 10000 mm, to analyze their influence on the stability of columns.

Column with short flanges

Figure 2 and Figure 3 present the results of the column buckling analysis for the member with the short flanges (column T_1), namely (i) the P_{cr} vs L curves, (ii) the GBT deformation modes participation in critical mode of columns instability and (iii) the column buckling mode deformed configuration of two short-to-intermediate columns – they were obtained with ABAQUS shell finite element code. The analysis of these figures it is possible to draw the following conclusions:

- i) The critical load (P_{cr}) of the columns decreases monotonically with the length (L).

- ii) For short lengths, the column's instability occurs in a local-torsion modes (deformation modes prevalent in unstable are 5, 6 and 4 modes), for intermediate lengths, in flexural-torsional modes (modes 4 and 3) and for larger lengths, in minor axis flexural mode (mode 3).
- iii) The great susceptibility for this columns of instability phenomena involving torsion is confirmed - mode 4 has a major participation for short-to-intermediate lengths (see Figure 3). However, the torsion curve approaches only the critical curve for short columns (for long columns, there is a clear deviation of two curves due to the increasing importance of flexural modes).
- iv) The very short columns instability mode has a strong component of local deformation since the web and the flange are different - the slender element (in this case, the web) conditions the section instability.

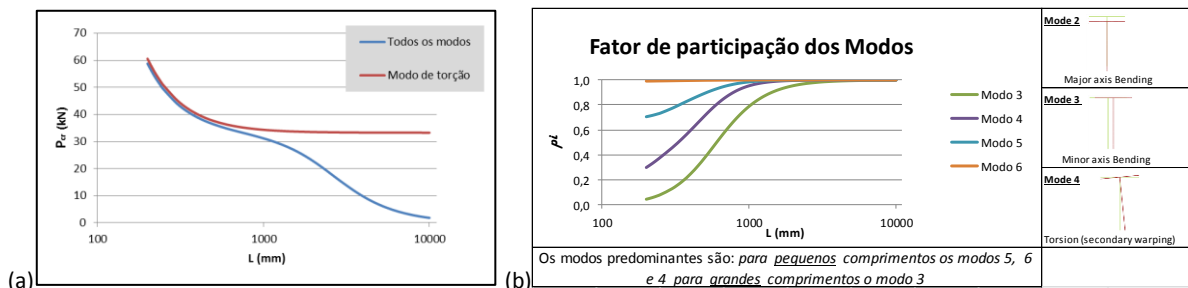


Figure 2: (a) P_{cr} vs. L curve and (b) GBT modal participation diagrams for T_1 columns.

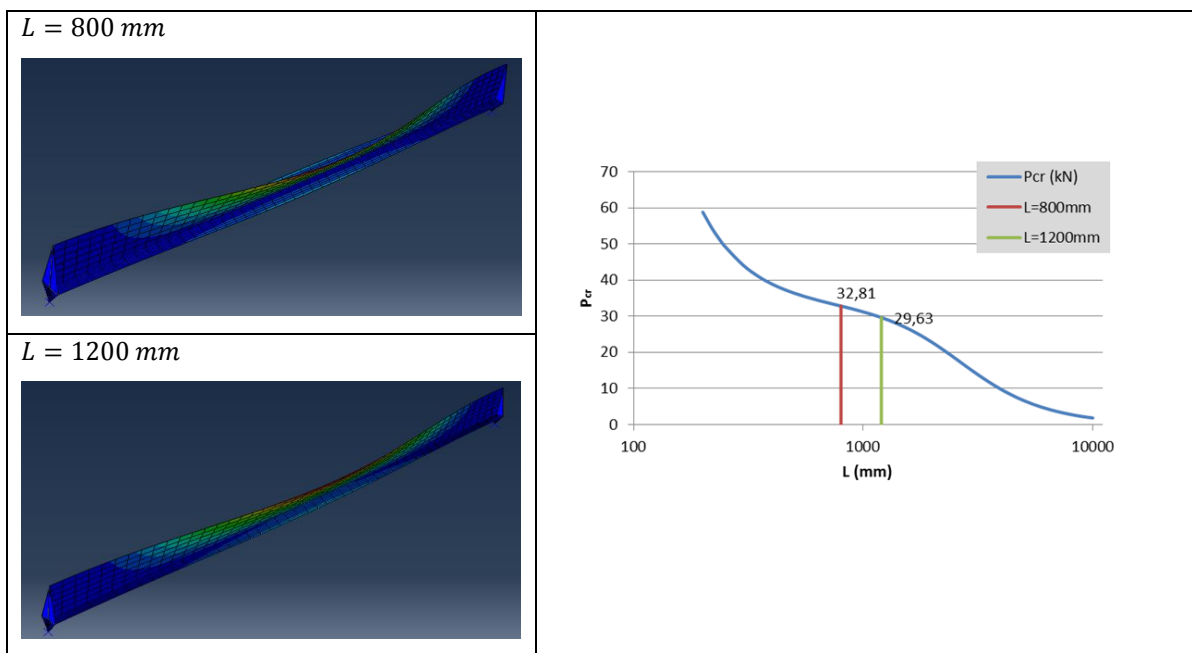


Figure 3: P_{cr} vs. L curve and deformed configuration for T_1 columns with 0.8 and 1.2m length.

A comparative analysis between sections T_1 and T_{12} noted that for short-to-intermediate lengths, the T_{12} the load plateau is virtually non-existent and the participation of minor axis flexure (mode 3) is more accentuated - e.g., two columns with length $L = 800$ mm columns buckle in flexural-torsional modes with the following characteristics: (i1) column in T_1 , modes 3 and 4 with 67.8% and 22.8%, (i2) column T_{12} , modes 3 and 4 with 94.76%, and 4.76%.

Finally, the thickness increase of the web increases critical load of column in a clearly way. For columns with $L = 800$ mm, a thickness increase from $t = 1.2$ up to $t = 2.4$ mm increased the 42% of the critical load.

Selected columns

The Selected lengths, based on linear stability analysis, were also important for the geometry of the columns selection, whose post-buckling behavior and ultimate resistance will be presented below with the selected values to allow to characterize the behavior of columns in plateau of P_{cr} vs L curves. Selected values are listed in Table 3 (a) and (b).

Table 3: Select length for (a) T_1 to T_7 and (b) T_{12} , T_{32} and T_{72} columns.

| | T_1 | T_2 | T_3 | T_4 | T_5 | T_6 | T_7 |
|---------|-------|-------|-------|-------|-------|-------|-------|
| $L(mm)$ | 600 | 800 | 800 | 800 | 800 | 800 | 800 |
| | 800 | 1100 | 1350 | 1600 | 1720 | 1720 | 1720 |
| | 1000 | 1300 | 1900 | 2400 | 2640 | 2640 | 2640 |
| | 1200 | 1700 | 2450 | 3200 | 3560 | 3560 | 3560 |
| | 1400 | 2000 | 3000 | 4000 | 4480 | 4480 | 4480 |
| | | 2300 | 3550 | 4800 | 5400 | 5400 | 5400 |
| | | 2600 | 4100 | 5600 | 6320 | 6320 | 6320 |
| | | 2900 | 4650 | 6400 | 7240 | 7240 | 7240 |
| | | | | 7200 | 8160 | 8160 | 8160 |
| | | | | | 9080 | 9080 | 9080 |
| | | | | | 10000 | 10000 | 9500 |
| | | | | | | | |

| | T_{12} | T_{32} | T_{72} |
|---------|----------|----------|----------|
| $L(mm)$ | 600 | 800 | 800 |
| | 800 | 1350 | 1720 |
| | 1000 | 1900 | 2640 |
| | 1200 | 2450 | 3560 |
| | 1400 | 3000 | 4480 |
| | | 3550 | 5400 |
| | | 4100 | 6320 |
| | | 4650 | 7240 |
| | | | 8160 |
| | | | 9080 |
| | | | 9500 |
| | | | |

Post Buckling Behaviour

The study of columns' post-buckling behavior was carried out using ABAQUS code [11]. The fixed ended columns analysed exhibit an initial imperfection with critical buckling mode with small amplitude (counterclockwise rotation with 30% of the wall's thickness value) – however, in the elasto-plastic analysis it was assumed a geometric imperfections combining two buckling modes: the critical flexural-torsional and the minor axis flexure mode, with amplitudes equal to 10% of the thickness and $L/1000$, respectively.

Elastic behaviour

Figure 4 to Figure 6 present the obtained results for column T_1 , short flange, in particular (i) the equilibrium trajectories P/P_{cr} vs. β (β is the torsion rotation in the mid span section), (ii) deformed post-critical ($P/P_{cr} \approx 1.2$) column's middle span section with $L = 600$ mm, (iii) the longitudinal profiles of the cutting centres displacement, according to the symmetry axis (d_s/t) and perpendicular to this axis (d_p/t), for columns with $L = 600$ mm and $L = 1400$ mm (positive displacement according to the reference of the figure). From The analysis of these figures it is possible to conclude:

- All columns display stable behaviors and significant post-buckling resistance. However, as the column length increases, the equilibrium trajectories $P/P_{cr}(\beta)$ become, progressively, more flexible.
- The longitudinal displacement profiles d_p/t and d_s/t , of column with 600 mm length exhibit a continuous evolution. The first curves have the deformed shape of a fixed ended column, so a central wave with "quarter-wave" to ensure null end slopes. This component has its origin in minor axis flexure component, which is associated to torsion, featuring the flexural and torsional mode of T-section columns with short flanges (the corresponding instability mode combines GBT modes 4 and 3).

- iii. This column displacement profiles d_s/t display null slope also at both ends (fixed ended consequence), but have three central half-waves and values clearly below to d_p/t - this displacement profile is usual for flexural and torsional behaviors (e.g., see [9]).
- iv. However, for the 1400 mm length column, these continuous progress, mentioned in the previous items, it is not verified. In fact, for values of relatively low load, the displacement profile d_s/t changes from three central half-waves for only one, displaying values substantially higher (five to ten times) to those verified for the short column – nevertheless, the values remain very inferior to their counterparts d_p/t . This behavior characteristic will be subject in a further analysis.

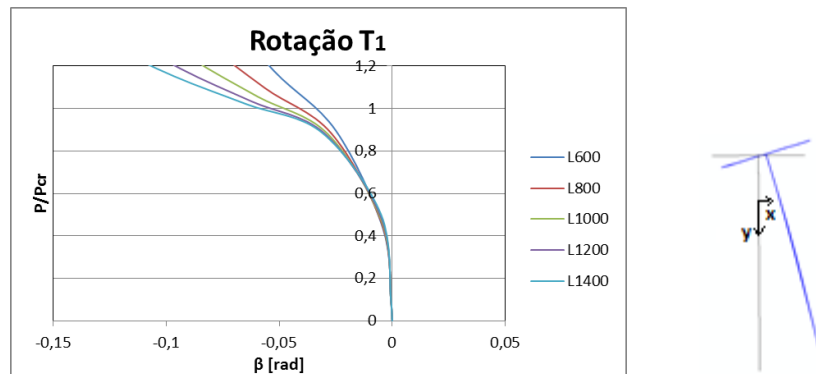


Figure 4: Post buckling trajectory, P/P_{cr} vs. β and mid-span deformed for T_1 ($L = 600\text{mm}$).

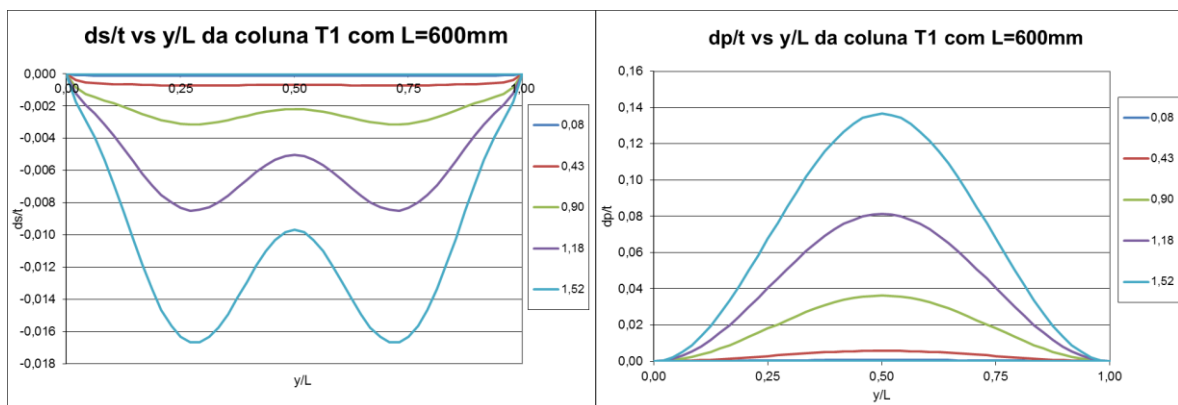


Figure 5: Longitudinal profiles of displacement d_s/t and d_p/t to T_1 column ($L = 600\text{mm}$) for different values of P/P_{cr} .

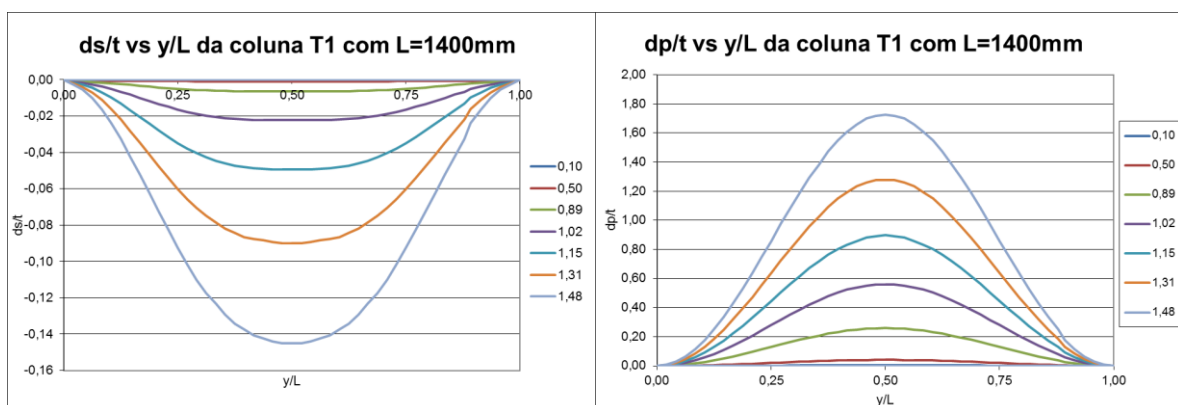


Figure 6: Longitudinal profiles of displacement d_s/t and d_p/t to T_1 column ($L = 1400\text{mm}$) for different values of P/P_{cr} .

- v. The behavior described earlier displays similar characteristics as the observed by Dinis et al. [9] in angles of equal legs and short-to-intermediate lengths submitted to compression. The authors showed that this behavior translates an interaction phenomenon between two modes of global instability: flexural and

torsional mode (on angles, modes 4 and 2 of GBT) and the minor axis flexure (3) - this interaction occurs as a result of two modes proximity in long columns.

- vi. The behavior described earlier displays similar characteristics as the observed by Dinis et al. [9] in angles of equal legs and short-to-intermediate lengths submitted to compression. The authors showed that this behavior translates an interaction phenomenon between two modes of global instability: flexural and torsional mode (on angles, modes 4 and 2 of GBT) and the minor axis flexure (3) - this interaction occurs as a result of two modes proximity in long columns.
- vii. Thus, the behavior of the T-section columns with short flanges and $L = 1400$ mm is associated an interaction phenomenon of with similar characteristics. Despite this, for these dimensions of the flanges, the flexural-torsion involves the flexural mode in lower inertia (4 and 3 modes of the GBT).
- viii. However, there is a behaviour feature in angles that it is not noted in the "T" section columns in the range of load values represented ($P/P_{cr} < 1,2$), do not occur equilibrium limits in the trajectories regarding longer columns.

In order to clarify the change in the displacements profile d_s/t mentioned in item (iv) of the previous comments, it is presented between Figure 7 and Figure 9 (i) post-critical deformed shape ($P/P_{cr} \approx 1,2$) of the mid-span section of columns with $L = 600$ mm and $L = 1400$ mm, and (ii) the distribution of normal strength (axial) of membrane in the mid-span with $L = 600$ mm and $L = 1400$ mm for different values of P/P_{cr} . From The combined observation of figures 4-6 and 7-9 it is possible to conclude:

- i. Post-critical deformed shape comparison between two columns allows to determinate that interaction between minor axis flexure mode causes a significant increase of displacement d_p , which makes (i1) almost double the mid-span rotation and therefore (i2) centroid changes up, i.e., causing negative displacements d_s .

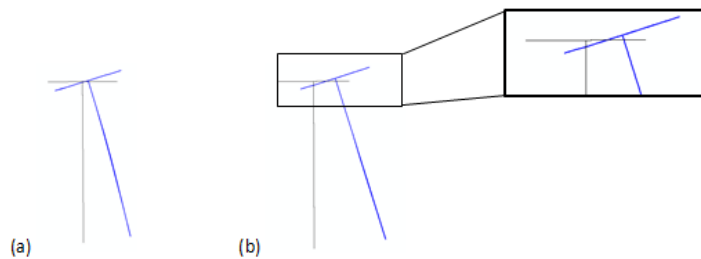


Figure 7: Post critical deformed of mid span T_1 columns with (a) $L=600$ mm and (b) $L=1400$ mm.

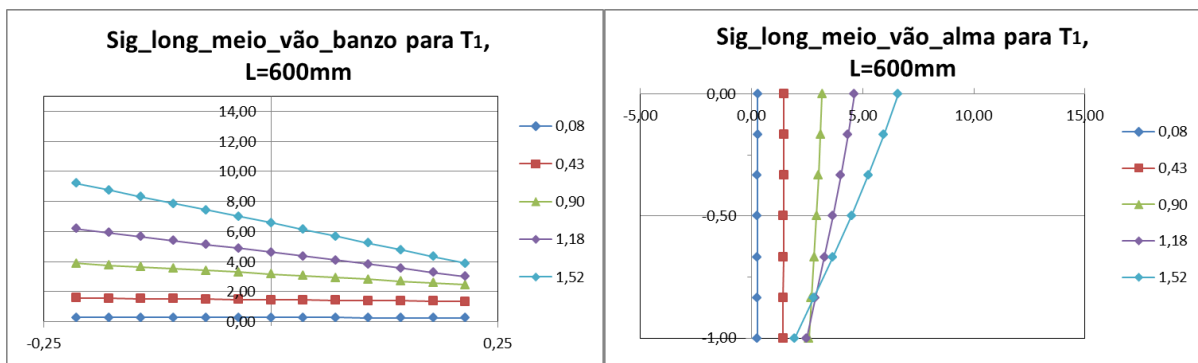


Figure 8: Normal strength distribution in the mid span section of T_1 ($L = 600$ mm) columns for different values of P/P_{cr} .

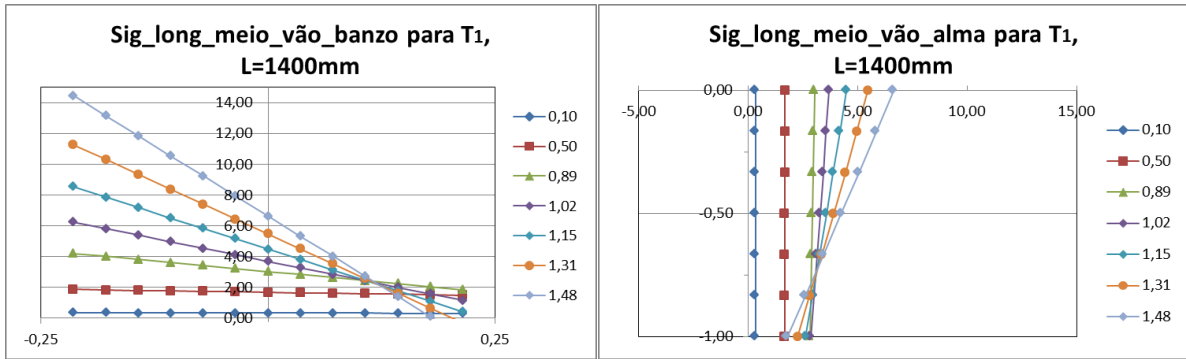


Figure 9: Normal strength distribution in the mid span section of T_1 ($L = 1400\text{mm}$) columns for different values of P/P_{cr} .

- ii. Being d_s caused by d_p displacements it is expected that (ii1) the first exhibits a similar progress as the latter (a central wave with "quarter-wave" outdoor to annul the slope at both ends), (ii2) its value grow quickly, crushing the three half-waves due to torsion (with a low value).
- iii. The existence of d_p and d_s displacements represents the presence of components, more or less important, minor or major axis flexural, respectively. Their presence can be detected by the normal strength diagram linear course, as in T-section column's web as in flange, which is a typical problem of skewed flexure.

Elasto-plastic behaviour

In this study it was admitted an elastic perfectly-plastic behaviour for steel (without taking into account the hardening, or the effect of residual strength) and four different values for the yield stresses: $f_y = 150, 300, 450$ and 600 MPa - to take into account a range of slenderness values ($\lambda = \sqrt{f_y/f_{cr}}$) between 1 and 4.

Figure 10 shows the post-buckling trajectory P/P_{cr} vs β of T_{12} columns with $L=800\text{mm}$ and $L=1400\text{mm}$, for the four tensile stress mentioned above - figure also indicates the elastic behavior trajectory. On the other hand, Figure 11 and Figure 12 show the plastic collapse deformations for yield stresses of 150 and 600 MPa. Finally, Table 4 presents the ratio f_u/f_y variation (f_u corresponds to the ultimate resistance/stress obtained in ABAQUS) with the slenderness of the columns. From these results analysis it can be concluded:

- i. For columns with short flanges (T_{12}) and $f_y/f_{cr} > 1$, exists some elasto-plastic resistance and ductility, particularly for lower yield stress values - in this case there is some deformation increment between the beginning of yielding and collapse, taking place in abrupt way for higher yield stress values.
- ii. For the column $L = 800$ mm there is a significant resistance with a yield stress increase - an increase of 33% and 57% of ultimate stress when the stress rises 100% f_y (300 MPa) and 300% (450 MPa), respectively.

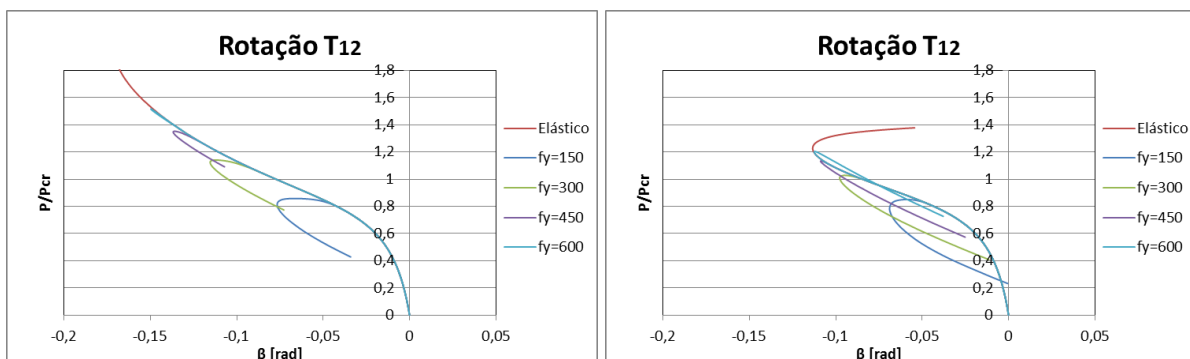


Figure 10: P/P_{cr} vs. β trajectory for four tensile stress of columns T_{12} ($L=800\text{mm}$ and $L=1400\text{mm}$).

- iii. However, this effect is less significant in longer columns – columns with $L = 800$ mm and $L = 1400$ mm, with resistance gains of 33% and 20%, respectively, when the yield stress is doubled (from 150 to 300MPa).
- iv. The plastic collapse deformation diagrams of T_{12} columns with $L = 800$ mm and $L = 1400$ mm show that the plastification is located mainly at the end of sections flange, near the mid-span, where the normal stress due to flexure is higher.

Figure 11 and Figure 12 illustrate the plastic deformed shape column with section T_{12} for the lengths $L = 800$ mm and $L = 1400$ mm and for yield stresses of 150 and 600 MPa, respectively.

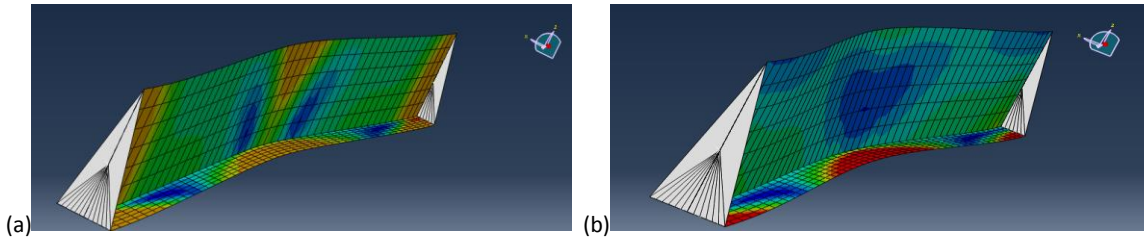


Figure 11: Plastic deformation the collapse of T_{12} columns ($L=800$ mm) with (a) $f_y = 150$ MPa and (b) $f_y = 600$ MPa.

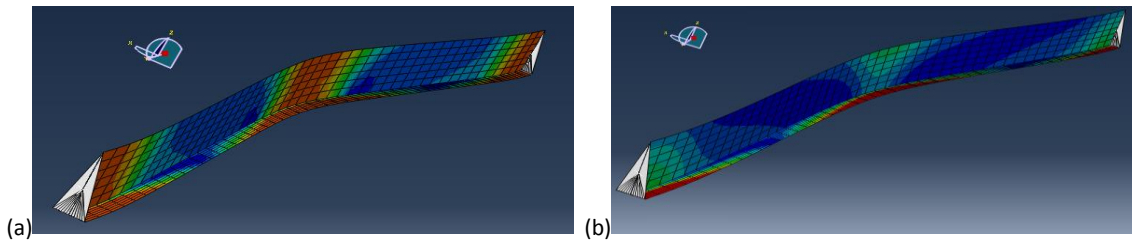


Figure 12: Plastic deformation the collapse of T_{12} columns ($L=1400$ mm) with (a) $f_y = 150$ MPa e (b) $f_y = 600$ MPa.

Table 4: Elasto-plastic ultimate load of T_{12} columns for $L=800$ and 1400 mm.

| f_y | T_{12} e $L=800$ mm | | | | T_{12} e $L=1400$ mm | | | |
|-------|-----------------------|-----------|------------|----------------|------------------------|-----------|------------|----------------|
| | f_u | f_u/f_y | f_{crit} | λ_{cr} | F_u | f_u/f_y | f_{crit} | λ_{cr} |
| 150 | 65,0 | 0,86 | 75,8 | 1,41 | 35,6 | 0,24 | 41,9 | 1,89 |
| 300 | 86,5 | 0,29 | | 1,99 | 43,0 | 0,14 | | 2,68 |
| 450 | 102,0 | 0,23 | | 2,44 | 47,5 | 0,11 | | 3,28 |
| 600 | 115,0 | 0,19 | | 2,81 | 50,4 | 0,08 | | 3,79 |

Direct Strength Method Design

This chapter evaluates the performance of the existing design curves of Direct Strength Method (DSM), originally proposed by Schafer [1-4]. The DSM consists in a set of Winter type curves, which calibration was based in a substantial number of experimental and numerical results, providing estimates for the ultimate resistance of cold formed steel columns and beams, whose collapse occurs in local modes (f_{nl}), distortional (f_{nl}), global (f_{ne}) or with local-global interaction (f_{nle}). For a more accurate evaluation of the performance of several strategies of DSM design the following figures represent the relation between the ultimate resistance, designated as "accurate", and the values obtained with the ABAQUS program, and the estimates provided by each of the three strategies of DSM, namely f_u/f_{nl} vs. λ_{cr} (Figure 13(a)), f_u/f_{ne} vs. λ_e and (Figure 13(b)), and f_u/f_{nle} vs. λ_{cr} (Figure 13(c)). From The observation of these figures it is possible to conclude the following:

- i) The estimated values by DSM local curve feature mostly, higher resistance values than values considered to be "accurate", which means that this estimate is not adequate and the local instability phenomena do not justify columns collapse.

- ii) This fact is confirmed by Figure 13(a), which clearly shows that the relationship between f_u/f_{nl} , mostly below 1.0, meaning that the resistance value estimated by f_{nl} is higher than the ultimate load of the column. In this case there was an average of 0.61 with a standard deviation of 0.25.
- iii) The DSM estimated values by the global curve are above the "real" values obtained with the ABAQUS. The estimates (see Figure 13(b)) overestimate substantially the columns resistance, in particular for low slenderness values - average equal to 0.65 and standard deviation of 0.17.
- iv) DSM curves on collapses with local-global interaction are clearly the best estimate for ultimate resistance of columns with T-section - there is a considerable number of results above 1.0.
- v) However, while the average of f_u/f_{nle} is 0.98 and display a standard deviation of 0.13, there is still a significant number of values lower than 0.8 - value considered as the lower limit acceptable.
- vi) Therefore, it can be concluded that the DSM resistance curves development for cold-formed steel T-section columns should be considered as a topic for future research.

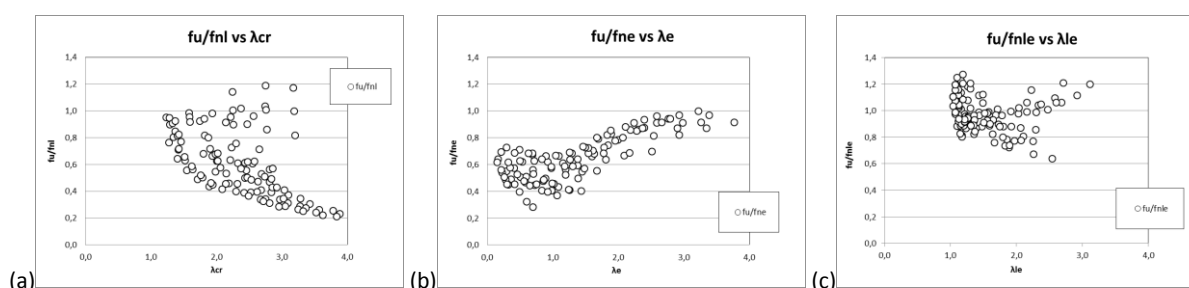


Figure 13: Variation of a) f_u/f_{nl} with λ_{cr} , (b) f_u/f_{ne} with λ_e and (c) f_u/f_{nle} with λ_{le} for T-sections columns.

Table 5: DSM: Average, standard derivation, maximum and minimum.

| MRD | Média | D. Padrão | Máximo | Mínimo |
|---------------|-------|-----------|--------|--------|
| f_u/f_{nl} | 0,61 | 0,25 | 1,19 | 0,19 |
| f_u/f_{ne} | 0,65 | 0,17 | 1,00 | 0,28 |
| f_u/f_{nle} | 0,98 | 0,13 | 1,27 | 0,64 |

Concluding Remarks

The conducted studies related to the buckling, post-buckling and ultimate resistance behaviors of cold-formed steel columns with T-section allowed several main conclusions.

In the buckling analysis it possible to deduct that the majority of the profiles with short-to-intermediate lengths buckle by flexural-torsion, with the flexural mode always associated to a perpendicular displacements to the axis of symmetry of the section (note that the sections are monosimétricas). In sections with short flanges the lateral flexure associated to torsion is in the minor inertia axis. In the smaller length columns the instability occurs essentially locally, while for the larger lengths the instability tendency is expressed in the minor inertia axis.

On post-buckling analysis, columns with small flanges have stable equilibrium trajectories once they do not present any "inversion" elastic points in the studied values range ($-0.15 < \beta < 0$). As the tensile stress increases, the ultimate load increases, however, this increase does not occur always in the same proportion. Note that for $f_y = 150MPa$ the ultimate load is lower than the critical load. However, for the remaining values the ultimate load is always higher than the critical load.

The DSM methodology that provides more precise estimates for the ultimate resistance for T-sections corresponds to consider local-global interaction. With an average value of 0.98 and a standard deviation of 0.13, constitutes a

valid hypothesis for the T-section columns design of, according to the ultimate load values determined in the parametric study. However, there are still some results for which the estimates are unreliable. As so the identification of a new proposal for this column should be the subject of a future research.

References

- [1] Schafer BW, Pekoz T, "Direct Strength prediction of cold formed steel members using elastic buckling solutions", *Thin Walled Structures – Research and development*, Elsevier, 137- 144, 1998.
- [2] Schafer BW, "Progress on the direct strength method", *Proc. of 16th International Specialty Conference on Cold-Formed Steel Structures (Orlando, 17-18/10)*, 647-662, 2002.
- [3] Schafer BW, "Cold-formed steel design by the direct strength method: bye-bye effective width", *Proc. of SSRC Annual Technical Session & Meeting (Baltimore, 2-5/4)*, 357-377, 2003.
- [4] Schafer BW, "Review: the direct strength method of cold-formed steel member design", *Journal of Constructional Steel Research*, 64(7–8), 766–778, 2008.
- [5] North American Specification for the Design of Cold-Formed Steel Structural Members (AISI-S100-07), American Iron and Steel Institute (AISI), Washington DC, 2007.
- [6] Sydney-Wellington, *Cold-Formed Steel Structures, Standards of Australia and Standards of New Zealand*, 2005.
- [7] NBR 14762:2010. Design of cold-formed steel structures. Associação Brasileira de Normas Técnicas.
- [8] Dinis PB, Camotim D, Silvestre N. On the local and global buckling of angle, T-section and cruciform thin-walled members. *Thin-Walled Structures*, 48, 786-797, 2010.
- [9] Dinis PB, Camotim D, Silvestre N. On the mechanics of thin-walled angle column instability. *Thin-Walled Structures*, 52, 80-89, 2012.
- [10] Dinis PB, Camotim D. A novel DSM-based approach for the rational design of fixed-ended and pin-ended short-to-intermediate thin-walled angle columns. *Thin-Walled Structures*, 87(February), 158-182, 2015.
- [11] Simulia Inc. (2008). *Abaqus Standard (vrs. 6.7-5)*.
- [12] Leal D. Perfis de aço formados a frio compostos por dupla cantoneira com seção "T" submetidos à compressão. *Dissertação de Mestrado. Escola de Eng. de São Carlos da Universidade de São Paulo*, 2011.
- [13] Sena Cardoso F, Rasmussen KJR. The Behaviour and design of concentrically loaded T-section steel columns, *Journal of Structural Engineering (ASCE)*, 140, 7(July), 1-17, 2014.
- [14] Vishnuvardhan S, Samuel Knight GM. Behaviour of cold-formed steel single and compound plain angles in compression. *Advanced Steel Construction*, 4(1), 46-58, 2008.
- [15] Rasmussen KJR. Design of angle columns with locally unstable legs. *Journal of Structural Engineering (ASCE)*, 131(10), 1553–60, 2005.
- [16] ASTM: 370 - 92, "Standard Test Methods and Definitions for Mechanical Testing of Steel Products", 1996.
- [17] Bebiano R, Pina P, Silvestre N, Camotim D, "GBTUL – A GBT-Based Code for Thin- Walled Member Analysis", *Proc. of 5th Conference on Thin-Walled Structures – Recent Innovations and Developments (ICTWS 2008 – Brisbane, 18-20/6)*, Vol. 2, 1173-1180, 2008.
- [18] Ellobody E, Young B. Behavior of cold-formed steel plain angle columns. *Journal of Structural Engineering (ASCE)*, 131(3), 457–66, 2005.